Numerical Simulation of Cone-jet Formation in Colloid Thruster

IEPC-2009-191

Presented at the 31st International Electric Propulsion Conference,
University of Michigan • Ann Arbor, Michigan • USA
September 20 – 24, 2009

Chao-Jin Qin[1], Hai-Bin Tang[2], Hai-Xing Wang[3]
Beijing University of Aeronautics and Astronautics, Beijing, 100191, P.R. CHINA

and

Jiang-Hong Wu[4]
South China University of Technology, Guangzhou, 510641, P.R. CHINA

Abstract: A electrospray model based on CFD code is used to investigate the process of liquid cone-jet formation in colloid thruster. The shape of the liquid cone-jet, the electric field and the flow field in and outside the cone-jet, the charge density and electric force density at the liquid surface could be obtained utilizing this model. The evolution process of cone-jet formation with the ethylene glycol, formamide and ethanol as working liquid are investigated in this paper. It shows that the overall development processes of cone-jet with the applied potential are similar; there is the "swirl dynamo" inside the cone. The effects of applied potential on the shape of cone-jet are also investigated in this paper. It is shown that with the increase of applied potential, the jets become thinner for the case with a fixed flow rate of ethanol. The shapes of cone-jet obtained in this study are roughly consistent with the experimental results.

Nomenclature

Ca	=	capillary number
L	=	length of hydraulic
E	=	electric field
$\boldsymbol{F}$, $\boldsymbol{F_s}$	=	body force, and surface volume force
$\mathbf{n}$	=	normal vector
P	=	pressure
Q	=	liquid flow rate
z, r	=	axial and radial coordinate
R_1, R_2	=	curvature radii
Re	=	Reynolds number
t	=	time
$\mathbf{T_e}$	=	electric stress tensor
α	=	volume fraction
ε_r, ε_0	=	relative and absolute permittivity
U	=	velocity

[1] Graduate Student, School of Astronautics, qinchaojin@sa.buaa.edu.cn
[2] Associate Professor, School of Astronautics, thb@buaa.edu.cn
[3] Associate Professor, School of Astronautics, whx@buaa.edu.cn
[4] Associate Professor, pmjhwu@scut.edu.cn

$\mathbf{V}$ = velocity vector
We = Weber number
Φ = potential
κ = curvature
γ = surface tension coefficient
μ = viscosity
ρ, ρ_g, ρ_l = mass density, gas and liquid density
ρ_e = charge density

I. Introduction

Colloid thrusters working with ions or electrified droplets are gradually becoming an alternative technology of space micro-propulsion that demanded in missions requiring high position controllability, compactness and low power consumption, such as LISA Pathfinder[1,2], Emerald[3] and etc. A colloid thruster is an electrospray device that consists of a hollow needle-like emitter and one or more coaxial electrodes that are commonly termed extractor and accelerator. By applying sufficient voltage between the extractor and the emitter, the mildly conductive propellant deforms into a cone. A submicron-sized jet of propellant forms at the cone apex which subsequently breaks up into droplets colloids. To a large extent, the operation performance of colloid thruster can be dependent on the cone-jet formation processes.

It has long been known that strong electric fields can disrupt liquid surfaces. When a liquid is subject to a sufficiently strong electric field, the liquid surface, usually at the end of a capillary tube, deforms in response to the electrical forces and surface tension and then forms itself into a cone with a jet emanating from its tip. This is the so called cone–jet mode. For Newtonian fluids, the jet eventually breaks up into small droplets further downstream. Owing to extensive technological applications, such as agricultural and automotive sprays, targeted drug delivery systems and ink-jet printers, the physics of cone-jet electrospray has come under intense study in the last decades.

Many researchers have contributed to the understanding of this phenomenon after the pioneering scientific description by Zeleny[4, 5]. Zeleny photographed drops held at the end of capillary tubes when a high potential is applied and then he measured the potential at which they disintegrated owing to the formation of a pointed end from which issued a narrow jet. Taylor presented an electrostatic solution of the liquid cone. He showed that to sustain a stable liquid cone when no jet is present, the half angle of the cone must be 49.3°. Since then, many theoretical and experimental analyses, numerical efforts have been preformed with the intention to find the physics mechanism of electrospray[6−15].

In the present paper, we describe a two-dimensional axi-symmetric formulation of the flow and electric fields of the electrostatically driven meniscus through a capillary nozzle. Based on the governing equations and CFD code, a numerical method has been developed to calculate the shape of the liquid cone and resulting jet, the electric fields, and the charge density along the liquid surface. The gas-liquid flow in present work is identified as free surface flow. The approach to treat this free surface flow is VOF method. The liquid properties, liquid flow rate and electrode configuration are needed as input parameters for the model. The simulation results are then compared with experimental data.

II. Numerical Approach

The objective of this work is to simulate the formation of cone-jet process based on commercial CFD code. The governing equations used to simulate formation of cone-jet process include the fluid dynamic equations and electrodynamic equations. In this paper, these equations are solved in both gas and liquid region. Only laminar flow and electrostatic field are concerned in present model and no current flow are consider in this modeling. Neglecting the current does not influence the early development of the cone and the jet, as mentioned in Ref.10. The governing equations and numerical procedure are described as follows.

A. Governing equations

In liquid bulk and gas field, the flow field is governed by the Navier-Stokes equation and continuity equation. A laminar, axi-symmetric flow is described by the following equations.

Equation of continuity

$$\frac{D\rho}{Dt} + \rho\nabla\cdot\mathbf{V} = 0 \tag{1}$$

Equation of momentum

$$\rho \frac{D\mathbf{V}}{Dt} = -\nabla P + \mu \nabla^2 \mathbf{V} + \mathbf{F} \tag{2}$$

In these equations, **V** denotes the velocity vector; P is the pressure; **F**, the body forces identified as gravitation; ρ the density, and μ the dynamic viscosity.

The potential field governed by the Poisson's equation can be expressed as

$$-\nabla\left(\varepsilon_r \varepsilon_0 \nabla \Phi\right) = \rho_e \tag{3}$$

where Φ is the potential, ε_r, ε_0, the relative and absolute permittivity, ρ_e the charge density. The electrical relaxation time is small compared to the hydrodynamic time, the liquid bulk is quasi-neutral and free charges are confined to a very thin layer underneath the liquid-air interface[8]. Therefore, we can use the assumption that all free charges accumulate only at the liquid-surface. Eq.(3) will be simplified to Laplace's equation in gas field and liquid region

$$-\nabla \cdot \left(\varepsilon_r \varepsilon_0 \nabla \Phi\right) = 0 \tag{4}$$

The momentum equation describes a force balance of the surface tension, gravity, inertia and viscous stresses. The approach to combine the fluid dynamic equations and electrodynamic equation is to add electric force into the momentum equation. If $\mathbf{T_e}$ is used to represent electric stress tensor, Eq.(2) can be written as

$$\rho \frac{D\mathbf{V}}{Dt} = -\nabla P + \mu \nabla^2 \mathbf{V} + \mathbf{F} + \mathbf{F_s} + \nabla \cdot \mathbf{T_e} \tag{5}$$

On the interface, the free charge for conductive liquid or polarization charge for dielectric liquid would result electric stress. While in axi-symmetric coordinate electric stress tensor is defined as[11]

$$\mathbf{T_e} = \begin{pmatrix} T_{zz} & T_{rz} \\ T_{zr} & T_{rr} \end{pmatrix} = \begin{pmatrix} \frac{\varepsilon}{2}\left(E_z^2 - E_r^2\right) & \varepsilon E_z E_r \\ \varepsilon E_z E_r & \frac{\varepsilon}{2}\left(E_r^2 - E_z^2\right) \end{pmatrix} \tag{6}$$

The importance of surface tension effects is determined based on the value of two dimensionless quantities, the Reynolds number, *Re*, and the capillary number, *Ca*; or the Reynolds number, *Re*, and the Weber number, *We*. For $Re \ll 1$, the quantity of interest is the capillary number: $Ca=\mu U/\gamma$, and for $Re \gg 1$, the quantity of interest is the Weber number: $We=\rho L U^2/\gamma$. where U is the free-stream velocity, γ is the surface tension coefficient. Surface tension effects can be neglected if $Ca \gg 1$ or $We \gg 1$.

In the problem, the surface tension obviously is important and it can be written in terms of the pressure jump across the surface

$$\Delta P = \gamma\left(\frac{1}{R_1} + \frac{1}{R_2}\right) \tag{7}$$

where R_1 and R_2 are radii of curvature of the surface. The surface curvature is computed from local gradients in the surface normal at the interface in present CFD code[12]. Let **n** be the surface normal vector, defined as the gradient of α_l, the volume fraction of the liquid.

$$\mathbf{n} = \nabla \alpha_l \tag{8}$$

The curvature, κ, is defined in terms of the divergence of the unit normal, $\hat{\mathbf{n}}$

$$\kappa = \nabla \cdot \hat{\mathbf{n}}, \quad \hat{\mathbf{n}} = \frac{\mathbf{n}}{|\mathbf{n}|} \tag{9}$$

The force at the surface can be expressed as a volume force using the divergence theorem. It is the volume force that is the source term which is added to the momentum equation. It has the following form

$$\mathbf{F_s} = \gamma \frac{\rho \kappa \nabla \alpha_l}{0.5\left(\rho_l + \rho_g\right)} \tag{10}$$

In Hartmann and Yan' s paper[8,9], the potential is solved for the whole geometry including the nozzle but the flow field is solved only for the liquid cone jet starting from the nozzle tip. In this paper, the gas-liquid flow in the whole computation domain is solved simultaneously.

The VOF (volume of fraction) method is used to determine free surface. In this method, the volume fraction equation derived from a continuity equation is solved and then the value of VOF is used to determine the phases or the surface of the certain cell. If the value of VOF is 1, it means the cell fully filled with liquid. The gas-liquid interface can be determined by the value of VOF where its value lies between 0 and 1. The discretization scheme applied on volume fraction equation is a modified version of the High Resolution Interface Capturing. This Modified-HRIC scheme consists of a non-linear blend of upwind and downwind differencing and provides improved accuracy for VOF calculations when compared to second order and other schemes[12]. The properties appearing in the transport equations are determined by the presence of the component phases in each control volume. In a gas-liquid system, the subscripts *g* and *l* of the density means the gas or liquid density, the density in this cell can be calculated by:

$$\rho = \alpha\rho_l + (1-\alpha)\rho_g \tag{11}$$

All other properties (e.g., viscosity) are computed in this manner.

B. Numerical procedure

In the present model, the flow field and electric field are coupled through electric stresses. The fluid motions are influenced by electric field and surface charge through the electric forces. In turn, these motions modify the surface charge distribution along the interface through the shape of cone-jet and the velocity field. The electric potential field is determined by the surface charge distribution, and the motion may substantially change the value of the electric field.

Figure 1 shows a schematic of the present numerical model's procedure. In each time-step, the computation cycle starts by calculating the steady-state electric field in both liquid and gas domain by solving Eq.(3) or Eq.(4). Then the electric stress is calculated by using formula (6) and surface tension is computed by Eq.(11). The cone-jet shape and the flow field are updated through solving Eq.(5) and continuity equation. After the convergence of the calculations each time-step, the cone-jet shape is compared with the former one. If the change of the shape is small, the cone-jet is considered as in steady-state and the calculation is stopped. Otherwise the new shape is used as input for a new cycle of computation.

C. Geometry and Boundary conditions

An axi-symmetric geometry used in this study is depicted in Fig.2. This geometry in present form cannot deal with non-symmetric modes like multi-jets and whipping.

A dielectric liquid entered metallic capillary from inlet AB and then finally issues into the air in the form of jet from the capillary. A high voltage is applied between the BC (the top electrode), and DE (the bottom electrode) so that an external electric field is formed between them. Because the BH is metallic capillary, its eclectic potential is equal to that of BC. The liquid flow rate Q is an input parameter of this model. The boundary conditions are divided into electrostatic and hydrodynamic conditions. More detail of boundary conditions can be found in Table 1.

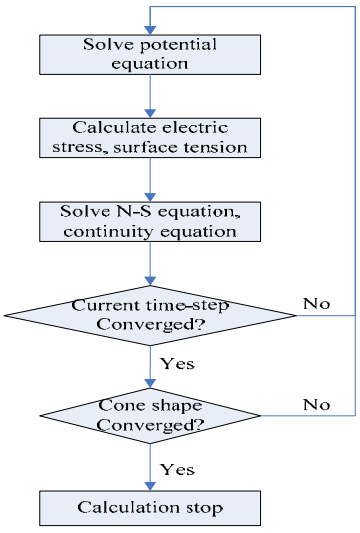

Figure 1. Flow chart of the calculation procedure

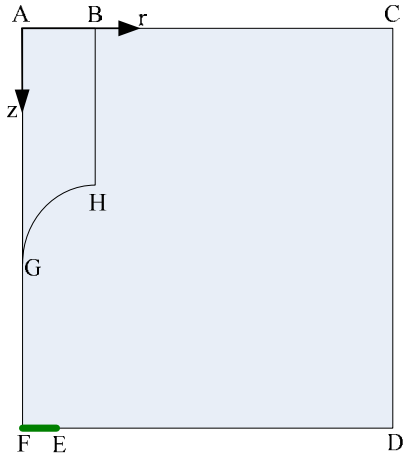

Figure 2. Computation domain

The calculations can have any shape of the liquid as initial condition, but in some previous results the gravity-driven meniscus was used. In present study, the initial shape of the liquid is flat surface at the capillary outlet. The surface tension and the body forces will deform the shape of the liquid at the outlet of capillary. This method is similar to the approach used by Lastow[10]. The liquid properties used in this study are listed in Table 2.

Table 1 Boundary condition values

Boundary	Electrostatic condition	Hydrodynamic condition	Case I(mm)	Case II(mm)	Case III(mm)
AB	$\nabla\Phi=0$	Q	4	0.125	0.0625
BC	$\Phi=U$	$P=0$	16	4	2
CD	$\nabla\Phi=0$	$P=0$	40	4	3
DE	$\Phi=0$	$P=0$	16	3	0.5
EF	$\Phi=0$	$P=0$	4	1	1.5
FA	$\nabla\Phi=0$	$P=0$	40	4	3
BH	$\Phi=U$	$P=0$	6	0.6	0.4
GH	$\Phi=U$	Q	N/A	N/A	N/A

Table 2 Liquid properties

Liquid	ε_r	γ (N/m)	μ (Pa·s)	ρ (kg/m^3)
Ethylene glycol	37	0.048	0.02	1109
Formamide+(1.73%w)NaI	111	0.058	0.0037	1153
ethanol	25	0.022	0.0016	789
Glycerol	45.8	0.0634	0.92	1262

III. Experimental System

In order to compare the modeling results with the experimental results, we also conduct the corresponding experimental studies. The experimental configuration is schematically shown in Fig.3. The emitter used in this experimental studies is stainless capillary with outer diameter is 0.5 mm, and inside diameter is 0.125 mm. An extractor electrode with a small orifice faces the emitter. The diameter of the extractor's orifice is 3 mm. The distance between the tip of emitter and the facing extractor is approximately 2.6 mm. The liquid is fed to the emitter through Nano Flowmeter. The flow rate of solution is measured by Nano Flowmeter and Differential Pressure Transducer. In order to monitor the cone-jet formed at emitter exit, a CCD Camera with microscope is used. The emitter is charged positive to extractor through a High voltage supplier which could supply applied potential of 10kV.

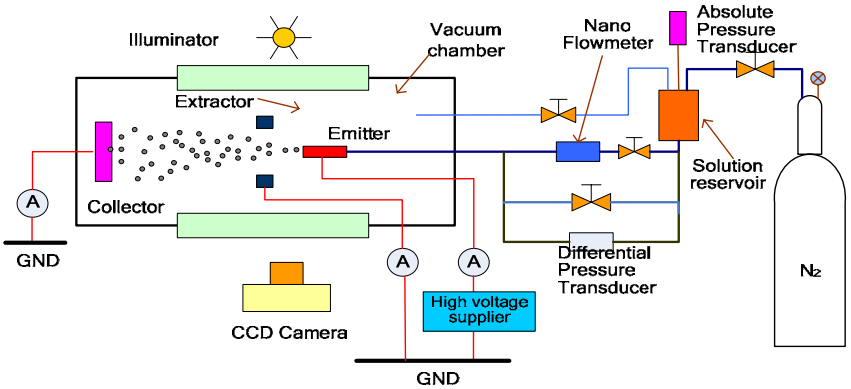

Figure 3. Sketch of the experimental set-up

IV. Results and Discussion

A. Results of ethylene glycol atomization

To confirm the availability of CFD-based model simulating the process of cone-jet formation, a configuration of numerical model which was similar to the experimental arrangement used by Hartman et al. was employed in our modeling firstly[8]. The configuration comprised a metallic capillary with diameter of 8 mm and a plate with radius of 20 mm. There is a hole with diameter of 8 mm in the center of plate as the counter electrodes. More detail of this configuration can be found in column "Case I" in table 1. The liquid used was ethylene glycol, and its properties were given in Table 2[8].

Figure 4(a) shows the shape of a cone-jet of ethylene glycol for the case that the liquid flow rate is $1.4\times10^{-9}m^3s^{-1}$ and the applied potential difference is 20 kV. The pressure of air is 1 atm. The experimental data and modeling result under the same condition from Hartman are shown in Fig.4(b) and Fig.4(c). It shows that the predicted cone-jet shape in our modeling agrees well with Hartman's simulation and experimental results. The result also roughly consistent with Yan's modeling results.

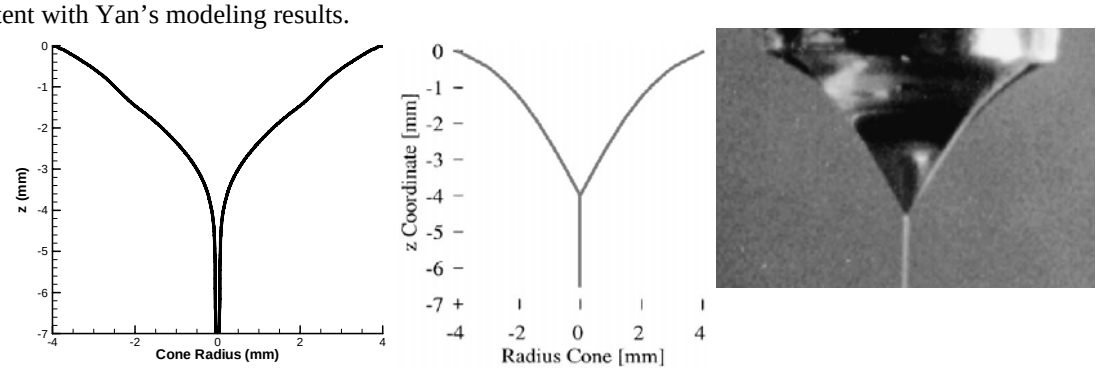

(a) (b) (c)

Figure 4. Comparison of calculated results of the cone-jet shape with experimental data.

The electric field varies with time due to the deformation of liquid shape and the changing of velocity field. The distribution of electric field in both gas and liquid region at the steady-state are shown in Fig. 5. It is found that there is electric field inside liquid cone-jet due to the liquid is dielectric and electric strength become intense in cone-jet transition region.

In equilibrium state, the free charges are confined to liquid surface (shown in Fig.6(a)) and could achieve to 13 C/m^3. Figure 6(b) shows distribution of the electric force density and illustrates that the distribution coincide with the charge density distribution. The electric force density at the surface almost reaches 17 MN/m^3.

Figure 7(a) shows the velocity distribution inside the cone-jet. Figure 7(b) shows the velocity magnitude distribution along the interface of gas-liquid and the axis. The surface velocity is accelerated rapidly from almost zero at the capillary tip to 1 m/s at the cone apex due to the electric stress and gravity. Because of viscosity and the gravity, velocity inside the cone-jet is also accelerated and the surface velocity is always larger than the velocity at the centerline. As the jet develops the velocity profile inside the jet become almost uniform.

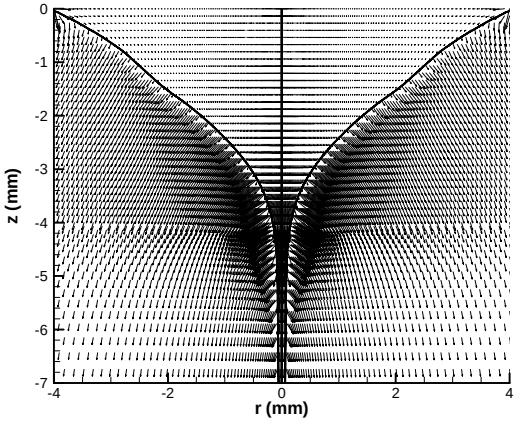

Figure 5. Electric field distribution in gas and liquid region.

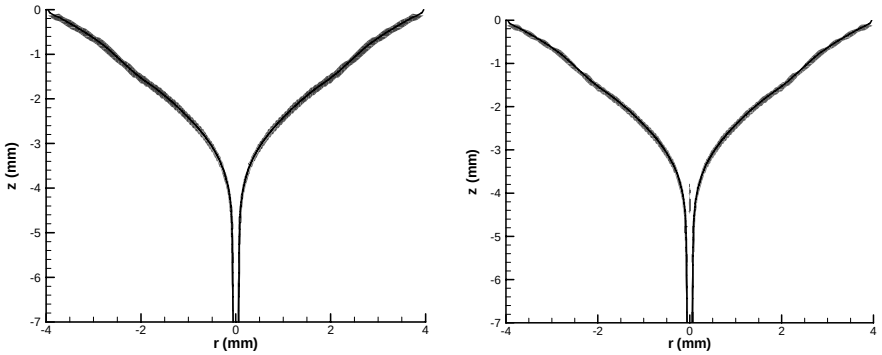

(a) Charge density, ρ_e=0~13C/m^3 (b) Electric force density, $|\nabla \cdot \mathbf{T_e}|$=0~17MN/m^3

Figure 6. Distribution of charge density and electric force density in computation domain with applied voltage 20kV and flow rate 1.4×10^{-9} m^{3}s^{-1}.

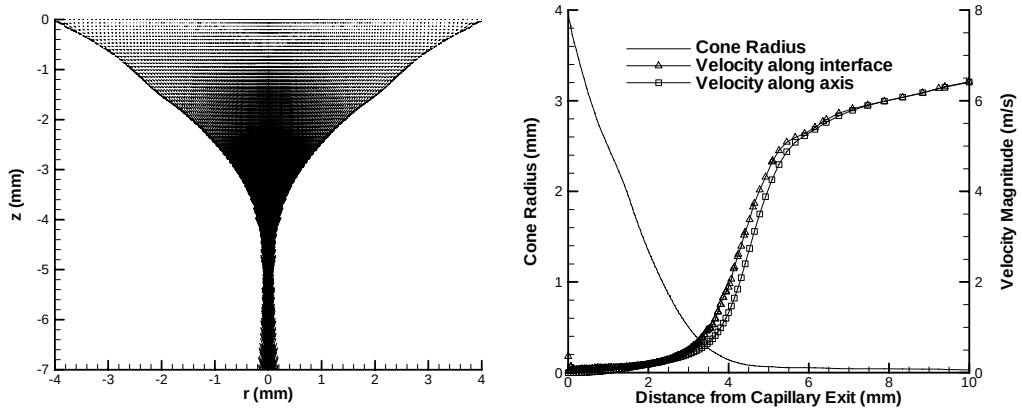

(a) (b)

Figure 7. (a)Velocity field distribution in liquid bulk; (b)Variation of velocity magnitude along the air-liquid interface.

B. Results of other liquid atomization

The set-up configuration used in this simulation is similar to the experimental studies. The properties of mixture of formamide and NaI are given in Table 2[13]. The capillary's diameter is 0.25 mm and the distance between the tip of capillary and extractor is 3.4 mm. More detail of the configuration is shown in column "Case II" in table 1. The gas is air with the pressure of 1 atm. The flow rate is set to be 6 μl/min and the applied voltage is 5000 V.

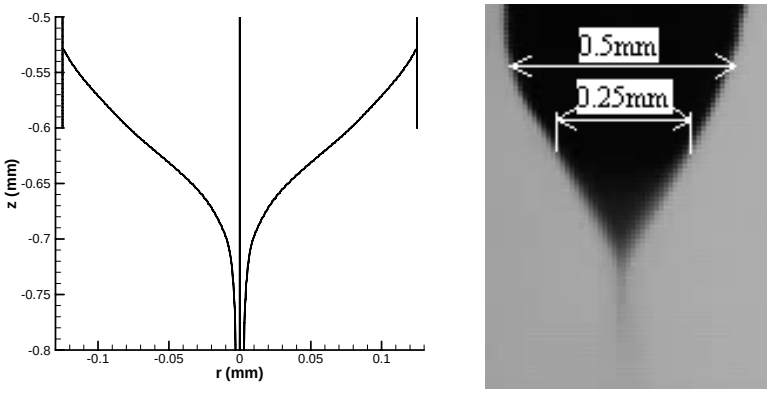

Figure 8. Comparison of calculation results of the cone-jet shape with experimental data

Figure 8 shows the shape of the cone-jet of numerical outcome and experimental result. The left figure shows the predicted shape of liquid cone and right figure is the experimental photo for the same condition. It can be seen that the predicted shape of cone jet is very similar to that of experimental results.

Figure 9(a) gives the electric potential contours in the whole domain and the electric field distribution is depicted in Fig.9(b). The location of capillary is also indicated in the figure. Due to the deformation of liquid shape, the potential contours also deform along the free surface.

During the formation process of cone-jet, some striking features can be found inside and outside the liquid. Figure 10 shows the formation and development of "swirl dynamo" inside the cone with time. Firstly, the flow is laminar under the effects of body force and electric stress (shown in Fig.10 (a)). Next, due to a cumulative effect of motion converging to the apex near the surface, the flow is collapsed—strong near-axis bipolar jets appeared (shown in Fig.10 (b)). In the next stage, a swirl would be generated as a result of bifurcation (shown in Fig.10(c)). Further more, the swirling flow would be separated depending on Re of liquid flow. This phenomenon is called vortex breakdown. This process is similar to Shtern and Barrero's analysis and observation results[14, 15].

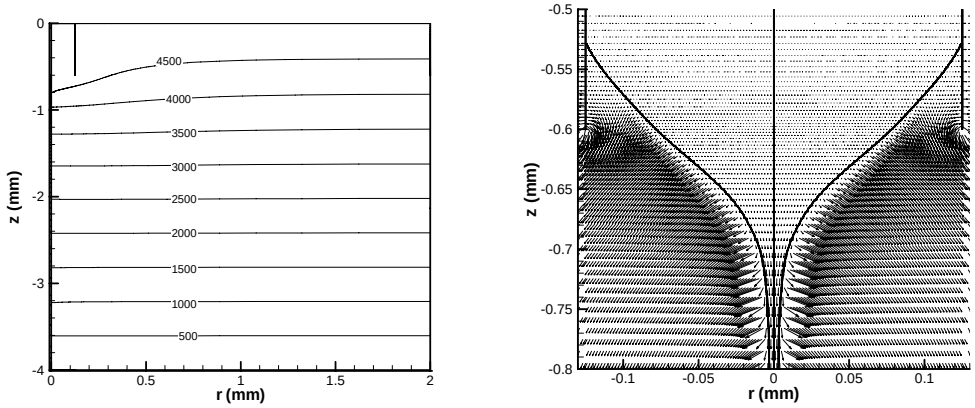

(a) (b)

Figure 9. (a) Potential contours for applied voltage 5 kV with flow rate 6 μl/min; (b) Electric field distribution in gas and liquid region.

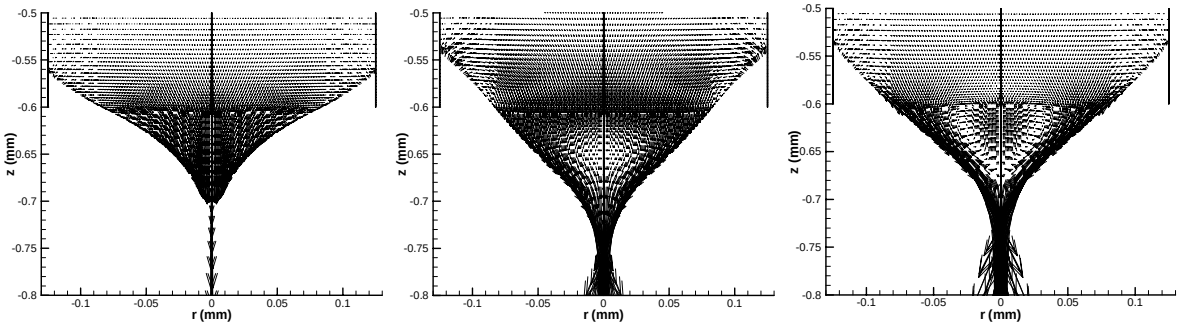

(a)t=0.07ms (b) t=0.17ms (c) t=0.30ms

Figure 10. Velocity field distribution in liquid region during cone-jet formation process.

Figure 11(a) shows the variation of the axial velocity along the interface of cone jet and the axis at steady state. Due to the tangential electric stress, axial velocity at the surface is accelerated rapidly from almost zero at the nozzle tip to about 3 m/s at the cone apex for this case. The velocity keeps on increasing gradually along the jet also due to the reduction of the jet radius. Axial velocity along the axis become negative inside cone is obliviously found in the Fig.11(a) and Fig.10(c). The flow in liquid will induce the flow in gas region due to the electric stresses and viscous effects in gas-liquid interface. Figure 11(b) shows the flow field in gas region at steady state. It is found that velocity along the cone-jet surface is rapidly accelerated and a vortex also generated near the cone-jet transition region.

The development of cone-jet for the case with ethanol as working liquid is also investigated in this paper. In this case, the flow rate is fixed to be 0.25 ml/min but the different potential is applied. The configuration of experiment and simulation used is "Case III" in Table 1. Figure 12 shows that the velocity field in ethanol region for the case with applied potential 4 kV. Similar to the cases with the formamide solution as working liquid, the swirl flow inside the cone is obviously observed.

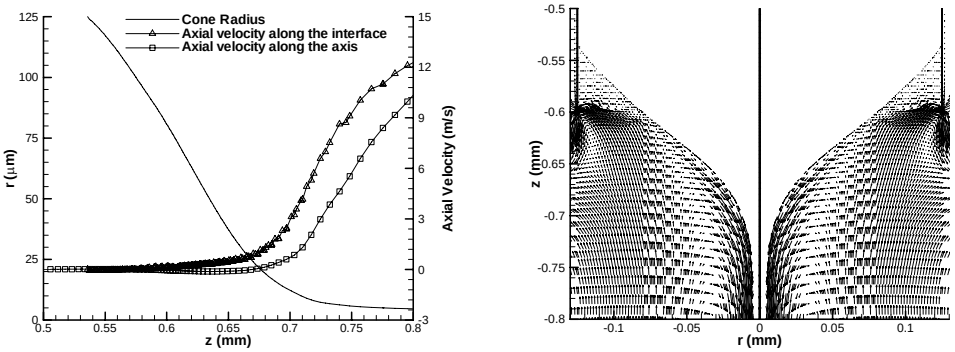

(a) (b)

Figure 11. (a) Axial velocity distribution along the interface and the axis; (b) Velocity distribution in gas field.

With applied potential increasing from zero, the cone-jet shape would become stable and approach to conical cone with slim jet. But if the applied potential exceeds certain value, the cone-jet will not stable anymore. Figure 13 shows the variation of cone-jet shape with the applied potential. It shows that with the increase of applied potential, the jets become thinner for the case with flow rate 0.25 ml/min. The prediction of voltage range is agreed well with the experimental data shown in Fig.13.

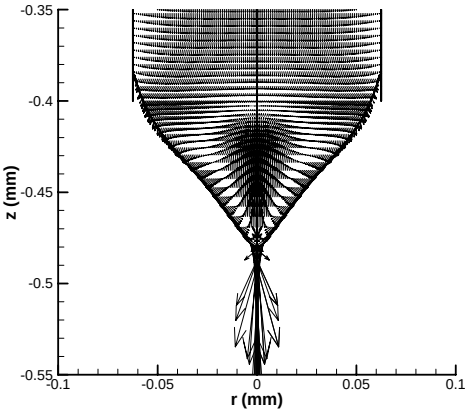

Figure 12. Velocity field inside cone-jet for ethanol with flow rate 0.25ml/min and applied potential 4kV

V. Results and Discussion

In this work, we present a comprehensive model used to describing the formation of cone-jet in colloid thruster based on CFD code. The governing equations were solved both in gas and liquid region. The hydrodynamic equations and electrostatic equations were coupled through the electric stresses acting on the liquid. The model is able to calculate the cone-jet shape and flow field in both liquid and gas domain. Numerical modeling for the cases with formamide and ethanol as working liquid, it shows that the overall development processes of cone-jet with the applied potential are similar; there is the "swirl dynamo" inside the cone. The surface velocity and dynamic pressure are accelerated rapidly from almost zero at the capillary tip to 6m/s at the cone apex due to the electric stress for the case with ethylene glycol as working liquid. The effects of applied potential on the shape of cone-jet are also investigated in this paper. It is shown that with the increase of applied potential, the jets become thinner for the case with a fixed flow rate of ethanol.

The neglecting of current conservation in the problem seems to have weak effect on the simulation results. But it should be used to investigating the current generation of free charges from liquid bulk with low electric conductivity. The prediction of droplet diameter and current flow generated from this electrostatically driven flow would be a study direction in the future. The axi-symmetric geometry cannot deal with non-symmetric modes like multi-jets and whipping. In further study, a 3D model would be developed to investigate these phenomena.

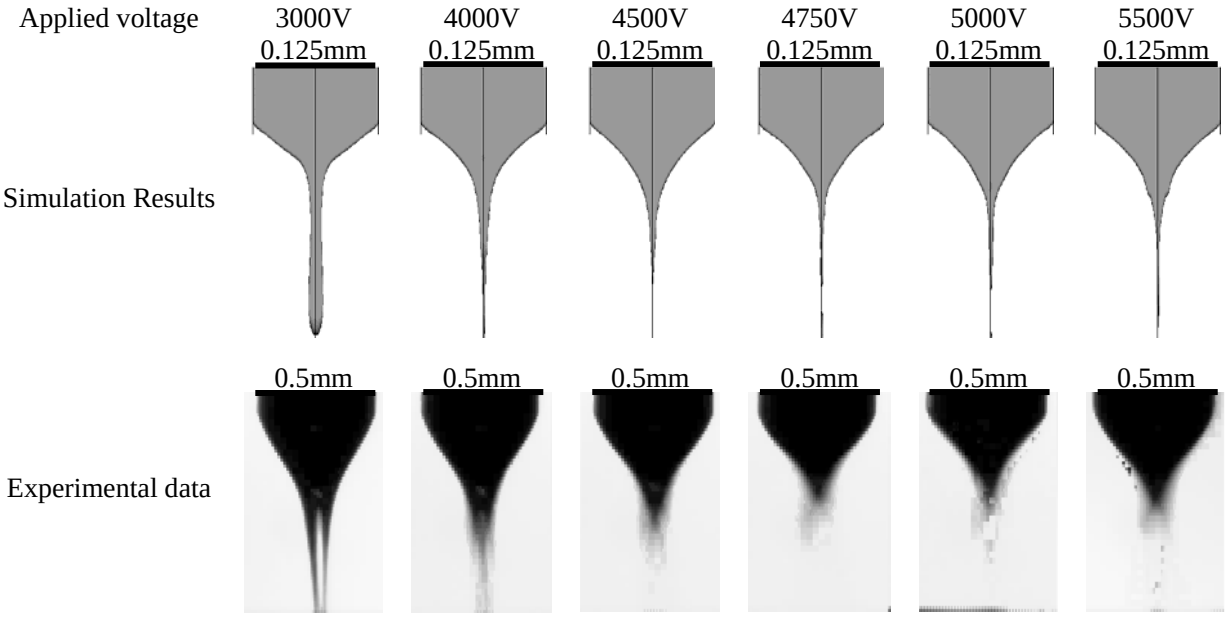

Figure 13. Cone-jet shape under different applied potential with flow rate 0.25ml/min.

References

[1]Buldrini, N., Genevese, A. and Tajmar, M., "In-FEEP cluster for LISA Pathfinder", IEPC, 2005, 22

[2]Ziemer, J.K. and Merkowitz, S.M., "Microthrust propulsion for the LISA mission", AIAA, 2004, 3439

[3]Pranajaya, F.M. and Cappelli, M.A., "Development of a colloid micro-thruster for flight demonstration on the emerald nanosatellite", AIAA, 2001, 3330

[4]Zeleny, J., "The electrical discharge from liquid points and a hydrostatic method of measuring the electric intensity at their surface", *Physical Review*, 1914, 3, 69—91

[5]Zeleny, J., "Instability of electrified liquid surfaces", Physical Review, 1917, 10, 1—16

[6]Taylor, G.I., "Disintegration of water drops in an electric field", *Proceedings of the Royal Society*, London, A, 1964, 280, 383—397

[7]Shtern, V., and Barrero, A., " Striking features of fluid flows in Taylor cones related to electrosprays", *Journal of Aerosol Science*, 1994, 25 (6), 1049–1063.

[8]Hartman, R.P.A., Brunner, D.J., Camelot, D.M.A., Marijnissen, J.C.M. and Scarlett, B., "Electrohydrodynamic atomization in the cone-jet mode physical modeling of the liquid cone and jet", *Journal of Aerosol Science*, 1999, 30(7), 823—849

[9]Yan, F., Farouk, B. and Ko, F., "Numerical modeling of an electrostatically driven liquid meniscus in the cone–jet mode", *Journal of Aerosol Science*, 2003, 34, 99—116

[10]Lastow, O. and Balachandran, W., "Numerical simulation of electrohydrodynamic (EHD) atomization", *Journal of Electrostatics*, 2006, 64, 850—859

[11]W. F. Hughes, E. W. Gaylord. *Basic equations of engineering science*, McGraw-Hill Inc, 1964

[12]*General Multiphase Models*, FLUENT 6.2 User's Guide, 2005

[13]Gamero-Castaño, M. and Hruby,V., "Electrospray as a source of nanoparticles for efficient colloid thrusters", AIAA, 2000, 3265

[14]Shtern, V. and Barrero, A., "Bifurcation of swirl in liquid cones", *Journal of Fluid Mechanic*s, 1995, 300, 169—205

[15]Barrero, A., Gañán-Calvo, A.M. Dávila, J., Palacios, A. and Gómez-González, E, "The Role of the Electrical Conductivity and Viscosity on the Motions inside Taylor Cones", *Journal of Electrostatics*, 1999, 47, 13—26

[16]Gañán-Calvo, A.M. and Barrero, A., "A global model for the electrospraying of liquids in steady cone-jet mode", *Journal of Aerosol Science*, 1996, 27, 179—180